

Published in final edited form as:

*Cancer Biol Ther.* 2009 March ; 8(5): 452–457.

## Diversity of DNA damage response of astrocytes and glioblastoma cell lines with various p53 status to treatment with etoposide and temozolomide

Yuichi Sato<sup>1,2</sup>, Akira Kurose<sup>1,\*</sup>, Akira Ogawa<sup>2</sup>, Kuniaki Ogasawara<sup>2</sup>, Frank Traganos<sup>3</sup>, Zbigniew Darzynkiewicz<sup>3</sup>, and Takashi Sawai<sup>1</sup>

<sup>1</sup>Department of Pathology; Iwate Medical University School of Medicine; Morioka, Iwate Japan

<sup>2</sup>Department of Neurosurgery; Iwate Medical University School of Medicine; Morioka, Iwate Japan

<sup>3</sup>Brander Cancer Research Institute; New York Medical College; Valhalla, New York USA

### Abstract

Phosphorylation of histone H2AX is a sensitive marker of DNA damage, particularly of DNA double strand breaks. Using multiparameter cytometry we explored effects of etoposide and temozolomide (TMZ) on three glioblastoma cell lines with different p53 status (A172, T98G, YKG-1) and on normal human astrocytes (NHA) correlating the drug-induced phosphorylated H2AX ( $\gamma$ H2AX) with cell cycle phase and induction of apoptosis. Etoposide induced  $\gamma$ H2AX in all phases of the cell cycle in all three glioblastoma lines and led to an arrest of T98G and YKG-1 cells in S and G<sub>2</sub>/M. NHA cells were arrested in G<sub>1</sub> with no evidence of  $\gamma$ H2AX induction. A172 responded by rise in  $\gamma$ H2AX throughout all phases of the cycle, arrest at the late S- to G<sub>2</sub>/M-phase, and appearance of senescence features: induction of p53, p21<sup>WAF1/CIP1</sup>, p16<sup>INK4A</sup> and  $\beta$ -galactosidase, accompanied by morphological changes typical of senescence. T98G cells showed the presence of  $\gamma$ H2AX in S phase with no evidence of cell cycle arrest. A modest degree of arrest in G<sub>1</sub> was seen in YKG-1 cells with no rise in  $\gamma$ H2AX. While frequency of apoptotic cells in all four TMZ-treated cell cultures was relatively low it is conceivable that the cells with extensive DNA damage were reproductively dead. The data show that neither the status of p53 (wild-type vs. mutated, or inhibited by pifithrin- $\alpha$ ) nor the expression of O<sup>6</sup>-methylguanine-DNA methyltransferase significantly affected the cell response to TMZ. Because of diversity in response to TMZ between individual glioblastoma lines our data suggest that with better understanding of the mechanisms, the treatment may have to be customized to individual patients.

### Keywords

glioblastoma; temozolomide; etoposide; DNA double strand break; DNA damage; senescence; cell cycle

### Introduction

Many anticancer drugs target DNA causing its DNA damage. During the past two decades, analysis of DNA damage in individual cells has been essentially limited to a single-cell DNA gel electrophoresis technique ('comet' assay), in which the extent and length of the

comet's tail reports the severity of DNA damage.<sup>1</sup> In recent years, however, it became apparent that phosphorylation of histone H2AX, one of the variants of the nucleosome core histone H2A, can provide a reliable marker of DNA damage. Namely, DNA damage, particularly when it involves formation of DNA double strand breaks (DSBs), induces phosphorylation of histone H2AX on Ser-139; phosphorylated H2AX is defined as  $\gamma$ H2AX.<sup>2</sup>  $\gamma$ H2AX may also be a marker of other DNA lesions including ssDNA breaks. The phosphorylation takes place on H2AX molecules on both sides of DSBs along a megabase length of DNA.<sup>2</sup> DSBs generated during DNA fragmentation in the course of apoptosis also induce  $\gamma$ H2AX but degree of  $\gamma$ H2AX induction in apoptotic cells is greater compared to the primary DSBs induced by antitumor drugs or radiation.<sup>3-5</sup> The presence of  $\gamma$ H2AX in the cells can be detected immunocytochemically in the form of distinct nuclear  $\gamma$ H2AX immunofluorescent foci and each focus is considered to correspond to a single DSB.<sup>6,7</sup> This immunocytochemical approach made it possible to assay DNA damage and repair in situ, in the chromatin of individual cells.<sup>8</sup> Compared to the comet assay, the immunocytochemical approach is significantly more sensitive.<sup>4</sup> The use of multiparameter flow cytometry in measurement of  $\gamma$ H2AX immunofluorescence enables one to correlate DNA damage with cellular DNA content corresponding to the cell cycle phase. Determination of the cell cycle phase targeted by the drug is of importance in elucidation of the mechanism of the anticancer drug activity.

Glioblastomas, frequent and lethal brain tumors with a median survival shorter than 12 months, are treated with standard therapy consisting of surgical resection followed by radiotherapy and adjuvant chemotherapy using anticancer drugs such as alkylating agents, DNA topoisomerase inhibitors and platinum analogs. Although nimustine [1-(4-amino-2-methyl-5-pyrimidinyl) methyl-3-(2-chloroethyl)-3-nitrosourea; ACNU] or carmustine [1,3-bis(2-chloroethyl)-1-nitrosourea; BCNU] has been commonly prescribed, temozolomide (TMZ), which shows significant efficacy combined with radiotherapy, has replaced these nitrosoureas and is now routinely used for the treatment of glioblastoma.<sup>9</sup> TMZ, a DNA methylating agent, induces cytotoxicity resulting primarily from the formation of O<sup>6</sup>-methylguanine lesions.<sup>10,11</sup> During DNA replication, O<sup>6</sup>-methylguanine mispairs with thymine,<sup>12</sup> leading to activation of the mismatch repair (MMR) system. Although the MMR system removes thymine, this base can be reinserted and futile cycles of MMR induced by the continuous mismatches have been reported to lead to various outcomes, such as G<sub>2</sub> arrest, cellular senescence, DNA double strand breaks (DSBs) or apoptosis.<sup>13-15</sup> However, detailed mechanism of anticancer activity of TMZ remains to be elucidated.

In the present study, we conducted flow cytometric bivariate analysis of  $\gamma$ H2AX and DNA content in glioblastoma cell lines and normal human astrocytes (NHA) treated with TMZ. Since various path-ways that effect cell cycle progression (MGMT), the suicide DNA repair enzyme which can remove the methyl group on the O<sup>6</sup> position of guanine, has been shown determine the cytotoxic effect of TMZ,<sup>18</sup> expression of MGMT before and after treatment of TMZ was examined as well. In addition, we carried out the same analysis after treatment with etoposide, a DNA topoisomerase II (topo2) inhibitor. Etoposide is also being used to treat glioblastoma and was reported to generate DSBs during the transcription.<sup>19-21</sup> The cells treated with etoposide thus provided a positive control to assess whether the  $\gamma$ H2AX can be used as marker of induction of DSBs in glioblastoma cell lines. This is the first paper that presents analysis of DSBs induction vis-à-vis cell cycle phase in glioblastoma and NHA cell lines after treatment with anticancer drugs.

## Results

### Detection of H2AX phosphorylation and apoptosis after treatment with etoposide

Treatment with 23.5  $\mu\text{g/ml}$  etoposide led dramatic changes in the bivariate (DNA content vs.  $\gamma\text{H2AX}$ ) distributions (cytograms) of all three types of glioblastoma cell lines (Fig. 1). In A172 cells the induction of  $\gamma\text{H2AX}$  was seen in all phases the cell cycle by 12 h and this pattern persisted up to 72 h. Some A172 cells underwent apoptosis by 48 h as was evident by the presence of cells with fractional (sub- $\text{G}_1$ ) DNA content. Virtually all T98G and YKG-1 cells treated with etoposide induced high level of  $\gamma\text{H2AX}$  through all phases of the cell cycle by 12 h. Both cell lines demonstrated a marked S phase accumulation of cells with  $\gamma\text{H2AX}$  induction by 24–48 h though by 72 h the majority the remaining cells appeared to have a  $\text{G}_2/\text{M}$  phase DNA content. Apoptotic cells with sub- $\text{G}_1$  DNA content were present by 48 h and as apoptosis gradually progressed the intensity of  $\gamma\text{H2AX}$  induction was decreasing concurrently with the loss of DNA content of these sub- $\text{G}_1$  apoptotic cells.<sup>3-5</sup>

### Detection of $\gamma\text{H2AX}$ and apoptosis and alteration of the cell cycle after treatment with TMZ

Figure 2 illustrates the response of NHA and the three glioblastoma cell lines to 100  $\mu\text{M}$  TMZ in terms of the H2AX phosphorylation and effects on the cell cycle. NHA cells showed predominantly arrest at the  $\text{G}_1$  phase of the cell cycle, with a minor presence of  $\text{G}_2/\text{M}$  cells. Neither increase in  $\gamma\text{H2AX}$  nor a significant increase in frequency of apoptosis was detected following treatment of NHA cells. In A172 cells, H2AX phosphorylation was detected in all the cell cycle phases, and the late S- to  $\text{G}_2/\text{M}$ -phase arrest was evident by 72 h after the addition of TMZ. After 120 h, nearly all of A172 cells underwent the late S- to  $\text{G}_2/\text{M}$ -phase arrest and the presence of cells with DNA ploidy higher than 2 DI was seen after 168 h and 240 h. The level of  $\gamma\text{H2AX}$  in A172 cells remained high throughout 240 h of the treatment. In the case of T98G cells no significant changes in the cell cycle distribution were apparent and relatively few apoptotic cells were present throughout the treatment. Induction of  $\gamma\text{H2AX}$  in these cells was predominantly in the S phase, seen after 72 h and 120 h and then declining. YKG-1 cells showed arrest at the  $\text{G}_1$  phase, most pronounced after 120 h, with no evidence of significant H2AX phosphorylation. When after 120 h treatment with TMZ the medium was changed to the one without TMZ the data were essentially the same after further 120 h incubation compared to 240 h of the continuous TMZ treatment (data not shown).

Treatments with 12.5  $\mu\text{M}$  TMZ of all 4 cell lines showed the same response compared to those treated with 100  $\mu\text{M}$  TMZ (data not shown).

### Inhibition of p53 function

To determine whether p53 would be involved in the cellular response to TMZ, we studied the effect of the p53 inhibitor pifithrin- $\alpha$  on the treatment with TMZ.<sup>23,24</sup> The cells were pretreated with 50  $\mu\text{M}$  pifithrin- $\alpha$  for 1 h before the exposure to TMZ. Among the four types of cells, it is known that T98G and YKG-1 have mutant p53, whereas NHA and A172 cells have wild-type p53.<sup>25,26</sup> The pretreatment with 50  $\mu\text{M}$  pifithrin- $\alpha$  followed by the exposure to TMZ caused no significant alteration in the bivariate distributions of  $\gamma\text{H2AX}$  vs. DNA compared with those obtained after the treatment with TMZ only, in both NHA and A172 cells (data not shown).

Expression of the cell cycle-related proteins and MGMT after treatment with TMZ. Subsequently, we examined the expression of cell cycle related proteins, p53, p21<sup>WAF1/CIP1</sup>, p16<sup>INK4A</sup>, p27<sup>KIP1</sup> and cyclin E, and a checkpoint protein kinase 2 (Chk2), since those proteins are known to regulate cell cycle progression or are considered to be involved in the cellular response during DNA repair.<sup>16,17,27</sup> A172 cells, especially in S and  $\text{G}_2/\text{M}$  showed

nearly a doubling in expression of p53, p21<sup>WAF1/CIP1</sup> and p16<sup>INK4A</sup> after the treatment with TMZ for 120 h (Fig. 3). On the other hand the expression of these proteins was essentially unchanged in NHA and YKG-1 cells (not shown). However, the level of p53 and p16<sup>INK4A</sup> in T98G cells was lowered after treatment with TMZ (not shown). Expression of p27<sup>KIP1</sup>, cyclin E and Chk2 did not change after the treatment with TMZ for 120 h in any of the 4 types of cells (data not shown). Low levels of MGMT were detected throughout the cell cycle in all 4 cell lines in the absence of exposure to TMZ. The expression levels among the 4 types of cells were similar. Treatment with TMZ for 48 h did not alter the expression of MGMT in any of the 4 cell types examined (data not shown).

### Detection of senescence-associated $\beta$ -galactosidase after treatment with TMZ

Because A172 cells showed increased expression in p53, p21<sup>WAF1/CIP1</sup> and p16<sup>INK4A</sup>, known to be correlated with senescence,<sup>28-30</sup> we examined the expression of senescence-associated  $\beta$ -galactosidase in the glioblastoma cells. The three lines without TMZ treatment showed less than 5% of positivity for senescence-associated  $\beta$ -galactosidase. After the treatment with 100  $\mu$ M TMZ for 168 h, 70% of A172 cells were positive for senescence-associated  $\beta$ -galactosidase, whereas 20% of T98G and YKG-1 cells respectively were positive (Fig. 4). Morphologically, the nuclei of A172 cells showed enlargement and lobulation and the cytoplasm enlarged and flattened, which were consistent with those morphological changes seen in senescence,<sup>31</sup> whereas T98G and YKG-1 did not alter their shape.

### Discussion

The induction  $\gamma$ H2AX by etoposide or TMZ, which was presently measured in relation to the cell cycle phase by cytometry, and visualized on cell images as the presence of immunofluorescent foci, in all probability represents the induction of DNA damage involving formation of DSBs. Because many papers used concentrations of etoposide and TMZ, 23.5  $\mu$ g/ml and 100  $\mu$ M respectively, we also studied the drug effects with the same concentrations. However Zhou et al. showed that intratumoral TMZ concentration reached 12.5  $\mu$ M, then we also used 12.5  $\mu$ M TMZ and demonstrated the same effect compared with 100  $\mu$ M TMZ.<sup>32</sup> The presence of DSBs in the cells treated with etoposide in all phases of the cell cycle (Fig. 1) is consistent with the published mechanism of topo2 inhibitors action namely the induction of DSB during both the transcription as well as DNA replication.<sup>20,21</sup> This is in contrast to the results obtained with topoisomerase I inhibitors which generate DSBs predominantly during DNA replication.<sup>33,34</sup> It should be noted however that the response of T98G and YKG-1 cells to etoposide was distinctly different than A172 cells. The former two cell lines showed perturbed progression through S phase and after 48 h essentially all cells were arrested in S phase where they demonstrated high level of  $\gamma$ H2AX induction. In contrast, the A172 cells had distinct populations of G<sub>1</sub> and G<sub>2</sub>/M cells inducing  $\gamma$ H2AX even after 72 h of the treatment and there was no evidence of cell arrest in S phase. It is likely that as a result of the presence of wt p53 in A172 cells the initial induction of DNA damage by etoposide triggered p53 mediated upregulation of p21<sup>WAF1/CIP1</sup> that led to their G<sub>1</sub> arrest thereby preventing progression through S. No such arrest was apparent in the T98G and YKG-1 cell having mutated p53. The observed induction of apoptosis most likely was a consequence of extensive DNA damage as revealed by the formation of primary DSBs in all three glioblastoma cell lines treated with etoposide.

In the present study, treatment with TMZ led to different effects in each among the four cell lines studied. NHA responded by cell arrest in G<sub>1</sub> with no evidence of induction of H2AX phosphorylation. The A172 cells were not blocked in G<sub>1</sub> but slowly progressed through S, accumulated at the late S to G<sub>2</sub>/M phase (120–168 h), and then were entering higher DNA ploidy (240 h). Interestingly, these A172 cells were ultimately undergoing senescence as

evident by positivity for p53, p16<sup>INK4A</sup>, p21<sup>WAF1/CIP1</sup>, expression of senescence-associated  $\beta$ -galactosidase and morphological changes typical of senescing cells. The present study is thus the first to demonstrate that senescence-like changes, likely mediated by induction of DNA damage, do occur in glioblastoma cells treated with TMZ. It is of interest to note that the damage to DNA in A172 cell induced by etoposide (formation of “cleavable complexes” leading to DSBs; refs. 19-21) triggered their arrest in G<sub>1</sub> preventing progression through S (Fig. 1) while the damage by TMZ (DNA alkylation) did not stop them from S-phase traverse and in fact led to further accumulation of the damage and to senescence. The induction of p21<sup>WAF1/CIP1</sup> by TMZ in A172 cells, thus, was a sign of their senescence rather than a marker of G<sub>1</sub> arrest.

The senescence was seen only in A172 cell line among the four lines studied. Considering the possible association of functional p53 with the senescence in A172 cells, we pretreated NHA and A172 cells with pifithrin- $\alpha$  before the addition of TMZ. However pifithrin- $\alpha$  did not appear to change the effects observed with TMZ alone on those two cell lines. This observation along with the fact that TMZ had quite different effects on NHA and A172 cell lines, both of which contain proficient wt p53,<sup>26</sup> suggest that p53 does not seem to be the critical factor causing the different effects of TMZ.

Although the increase in frequency of apoptotic cells was observed in all three glioblastoma cell lines after 72 h of the treatment with TMZ, it was not clear that this mechanism was responsible for TMZ's induced cytotoxicity that may account for its anticancer effects. It should be noted that apoptosis is the transient event of variable duration and at the end of the apoptotic process the cells undergo total disintegration and become undetectable.<sup>35</sup> The frequency of apoptotic cells present in cultures maintained relatively long (e.g., 240 h), therefore, may not be a reliable marker of the rate of induction of apoptosis and thus may not represent the cumulative number of all cells that ultimately underwent apoptosis during this time interval.<sup>35</sup> Therefore, it is difficult to assess to what extent the presence of DSBs contributed to apoptosis during this rather long time period. It is likely, however, that the cells with such extensive DNA damage as it was seen in the case of TMZ-treated A172 cells, were reproductively dead, unable to continue extended proliferation.

A fraction of T98G cells in the S phase showed the presence of DSBs as revealed by high level of  $\gamma$ H2AX induction after 72 h and 120 h. However, a few such cells were apparent after 168 and 240 h. It is possible that the cells with DSBs underwent apoptosis and the new cells entering S phase after 168 h or 240 h were more resistant to the drug. It is also possible, although less likely, that the cells somewhat recovered (repaired DSBs) by 168 h despite a constant presence of the drug in the medium. YKG-1 cells demonstrated modest degree of arrest in G<sub>1</sub> without increase in DSBs. Thus, the responses of cells in terms of DSBs induction, cell cycle perturbation and apoptosis after treatment with TMZ were quite different for each of the cell line among the four lines studied.

The mechanism of TMZ-induced growth inhibition of glioblastoma cells are controversial. Although Roos reported that the inhibitory effect of TMZ depends on apoptosis,<sup>15</sup> many reports including our results are not fully compatible with this notion. There have been reports suggesting that induction of senescence plays a main role of growth inhibition after TMZ treatment.<sup>13,36</sup> Since A172 underwent senescence after the treatment with TMZ, our data concur with the view that the growth inhibitory effect of TMZ is associated, at least in some glioblastomas, with induction of senescence. In this case, the induction of senescence appears to be mediated by the continuing presence of DSBs which were observed at high intensity already after 72 h (Fig. 2).



For further understanding of the anticancer mechanisms of TMZ, it is important to study what determines the differences in cellular responses to the drug including cell arrest, the extent of DSBs, and whether senescence and repair of DSBs occurs. The possible determinants include p53 status, MGMT expression and the MMR system. Many reports indicate that the status of p53 determines the cellular response to TMZ.<sup>13,15,37,38</sup> However, our results show that p53 is not the sole determinant because: (i) NHA and A172, both have wild-type p53 yet demonstrated quite different responses, and (ii) pifithrin- $\alpha$  had no significant effect on the cellular responses after the TMZ treatment.

MGMT has been known to play an important role in the cellular responses after TMZ treatment *in vitro*.<sup>15,37,39</sup> MGMT gene silencing has been shown to correlate well with clinical outcome after TMZ treatments.<sup>40</sup> Moreover, absence or low levels of MGMT expression examined by immunohistochemical techniques has been associated with favorable prognosis.<sup>41,42</sup> Concerning MGMT, we found the same levels of MGMT expression throughout the cell cycle, which were not altered by TMZ in any of the four cell lines studied. Our results indicate that the expression levels of MGMT seem not to correlate with the cellular responses after the treatment with TMZ. Although a proficient MMR system is required for the action of TMZ, little has been known about the association of the MMR system and efficacy of TMZ in glioblastomas.<sup>15,43,44</sup> Further investigation is needed in this regard.

In summary, since the cellular responses to TMZ were so diverse and cell-type dependent in glioblastomas, further approaches have to be taken to explain the causes of these differences and the mechanism of TMZ action on these cell types. Because of this diversity in response, with better understanding of the mechanisms the treatment may have to be customized to individual patients. The present report is the first to explore the anticancer effects of TMZ focusing upon DSBs which may contribute to our understanding of the mechanisms of action of anticancer agents.

## Materials and Methods

### Cell culture and drug treatment

Glioma cell lines, A172 (wt p53) and YKG-1 (mutant p53) were obtained from Health Science Research Resources Bank, Osaka, Japan, and T98G (mutant p53) was obtained from DS Pharma Biomedical Co., Ltd., Osaka, Japan. They were grown in dishes (Becton Drive, Franklin Lakes, NJ) in Dulbecco's minimum essential medium supplemented with 10% fetal bovine serum (Cambrex Bio Science Walkersville Inc., Walkersville, MD), 100 units/ml penicillin (Meiji Seika Kaisha, LTD., Tokyo, Japan) and 100  $\mu$ g/ml streptomycin (Meiji Seika Kaisha, LTD.,). NHA (wt 53) were obtained from Cambrex Bio Science and grown in AGM medium (Cambrex Bio Science Walkersville Inc.,). All cell lines were maintained at 37°C in a humidified atmosphere of 5% CO<sub>2</sub> in air. The cultures were treated with etoposide (Sigma Chemical Co., St. Louis, MO) or TMZ (LKT Laboratories, St. Paul, MN) for different time intervals. TMZ and etoposide were dissolved in dimethyl sulfoxide (Sigma) in advance. The effect of p53 inactivation on TMZ sensitivity was assessed by pretreatment with 50  $\mu$ M pifithrin- $\alpha$  (Sigma) for 1 h before the addition of TMZ.

### Immunocytochemistry

Both the floating cells in the medium and the attached cells after trypsinization were collected and fixed with 1% methanol-free formaldehyde (Polysciences Inc., Warrington, PA) in PBS at 0°C for 15 min and post-fixed with 80% ethanol for at least 2 h at -20°C. The fixed cells were washed twice in PBS and suspended in a 1% (w/v) solution of bovine serum albumin (Sigma) in PBS to suppress non-specific antibody binding. The cells were then

incubated in 100  $\mu$ l of 1% BSA containing 1:100 diluted antiphospho-histone H2AX (Ser-139) monoclonal antibody (Upstate, Lake Placid, NY, USA) for 2 h at room temperature, washed twice with PBS and resuspended in 100  $\mu$ l of 1:20 diluted FITC-conjugated F(ab')<sup>2</sup> fragment of goat anti-mouse immunoglobulin (DAKO, Glostrup, Denmark) for 30 min at room temperature in the dark. The cells were then counterstained with 5  $\mu$ l/ml propidium iodide (PI) (Sigma) in the presence of 100  $\mu$ g/ml of RNase A (Sigma) for 30 min. The expression analyses of p53 (DO-7, DAKO, Glostrup, Denmark, 1:100), p16<sup>INK4A</sup> (F-12, Santa Cruz Biotechnology, Inc., Santa Cruz, CA, 1:50), p21<sup>WAF1/CIP1</sup> (DCS60, Cell Signaling Technology, Inc., Danvers, MA, 1:100), p27<sup>KIP1</sup> (SX53G8, DAKO, 1:50), cyclin E (HE12, Medical & Biological Laboratories, Co., LTD., Nagoya, Japan, 1:100), Chk2 [phospho-Chk2 (Thr-68), Cell Signaling Technology, 1:25] and MGMT (MT3.1, Upstate, 1:40) were performed in the same way as  $\gamma$ H2AX immunostaining.

### Fluorescence measurements by flow cytometry

The fluorescence of FITC (green) and PI (red) of the individual cells in suspension induced by excitation with a 488 nm argon ion laser was measured using a FACScan flow cytometer (Becton-Dickinson, San Jose, CA, USA). The green and red fluorescence from each cell were separated and quantified using standard optics and CELL Quest software (Becton-Dickinson). Ten thousand cells were measured per sample. All experiments were repeated at least three times.

### Senescence-associated $\beta$ -galactosidase staining

Senescence-associated  $\beta$ -galactosidase staining was performed at pH 6 in cultured cells with the senescence staining kit (Cell Signaling Technology Inc.) following the kit recommendations.<sup>22</sup> The kit detects  $\beta$ -galactosidase activity at pH 6, which is present only in senescent cells. Percentages of senescence-associated  $\beta$ -galactosidase-positive cells, which show development of blue color in their cytoplasm, were determined for each sample using a bright-field microscope.

### Acknowledgments

We thank Yuji Shibata for excellent technical assistance.

### References

- Ostling O, Johanson KJ. Microelectrophoretic study of radiation-induced DNA damages in individual mammalian cells. *Biochem Biophys Res Commun.* 1984; 123:291–8. [PubMed: 6477583]
- Rogakou EP, Pilch DR, Orr AH, Ivanova VS, Bonner WM. DNA double-stranded breaks induce histone H2AX phosphorylation on serine 139. *J Biol Chem.* 1998; 273:5858–68. [PubMed: 9488723]
- Huang X, Traganos F, Darzynkiewicz Z. DNA damage induced by DNA topoisomerase I- and topoisomerase II-inhibitors detected by histone H2AX phosphorylation in relation to the cell cycle phase and apoptosis. *Cell Cycle.* 2003; 2:614–9. [PubMed: 14504478]
- Huang X, Okafuji M, Traganos F, Luther E, Holden E, Darzynkiewicz Z. Assessment of histone H2AX phosphorylation induced by DNA topoisomerase I and II inhibitors topotecan and mitoxantrone and by the DNA cross-linking agent cisplatin. *Cytometry A.* 2004; 58:99–110. [PubMed: 15057963]
- Huang X, Halicka HD, Traganos F, Tanaka T, Kurose A, Darzynkiewicz Z. Cytometric assessment of DNA damage in relation to cell cycle phase and apoptosis. *Cell Prolif.* 2005; 38:223–43. [PubMed: 16098182]

6. Sedelnikova OA, Rogakou EP, Panyutin IG, Bonner WM. Quantitative detection of (125) IdU-induced DNA double-strand breaks with gamma-H2AX antibody. *Radiat Res.* 2002; 158:486–92. [PubMed: 12236816]
7. Rogakou EP, Boon C, Redon C, Bonner WM. Megabase chromatin domains involved in DNA double-strand breaks in vivo. *J Cell Biol.* 1999; 146:905–16. [PubMed: 10477747]
8. Banáth JP, Olive PL. Expression of phosphorylated histone H2AX as a surrogate of cell killing by drugs that create DNA double-strand breaks. *Cancer Res.* 2003; 63:4347–50. [PubMed: 12907603]
9. Stupp R, Mason WP, van den Bent MJ, Weller M, Fisher B, Taphoorn MJ, et al. European Organisation for Research and Treatment of Cancer Brain Tumor and Radiotherapy Groups; National Cancer Institute of Canada Clinical Trials Group. Radiotherapy plus concomitant and adjuvant temozolomide for glioblastoma. *N Engl J Med.* 2005; 352:987–96. [PubMed: 15758009]
10. Tisdale MJ. Antitumor imidazotetrazines—XV. Role of guanine O<sup>6</sup> alkylation in the mechanism of cytotoxicity of imidazotetrazinones. *Biochem Pharmacol.* 1987; 36:457–62. [PubMed: 3470008]
11. Baer JC, Freeman AA, Newlands ES, Watson AJ, Rafferty JA, Margison GP. Depletion of O<sup>6</sup>-alkylguanine-DNA alkyltransferase correlates with potentiation of temozolomide and CCNU toxicity in human tumour cells. *Br J Cancer.* 1993; 67:1299–302. [PubMed: 8512814]
12. Karran P, Marinus MG. Mismatch correction at O<sup>6</sup>-methylguanine residues in *E. coli* DNA. *Nature.* 1982; 296:868–9. [PubMed: 7040986]
13. Hirose Y, Berger MS, Pieper RO. p53 effects both the duration of G<sub>2</sub>/M arrest and the fate of temozolomide-treated human glioblastoma cells. *Cancer Res.* 2001; 61:1957–63. [PubMed: 11280752]
14. Günther W, Pawlak E, Damasceno R, Arnold H, Terzis AJ. Temozolomide induces apoptosis and senescence in glioma cells cultured as multicellular spheroids. *Br J Cancer.* 2003; 88:463–9. [PubMed: 12569392]
15. Roos WP, Batista LF, Naumann SC, Wick W, Weller M, Menck CF, et al. Apoptosis in malignant glioma cells triggered by the temozolomide-induced DNA lesion O<sup>6</sup>-methylguanine. *Oncogene.* 2007; 26:186–97. [PubMed: 16819506]
16. Zhao H, Traganos F, Darzynkiewicz Z. Kinetics of histone H2AX phosphorylation and Chk2 activation in A549 cells treated with topotecan and mitoxantrone in relation to the cell cycle phase. *Cytometry A.* 2008; 73:480–9. [PubMed: 18459160]
17. Stiff T, Walker SA, Cerosaletti K, Goodarzi AA, Petermann E, Concannon P, et al. ATR-dependent phosphorylation and activation of ATM in response to UV treatment or replication fork stalling. *EMBO J.* 2006; 25:5775–8. [PubMed: 17124492]
18. Gerson SL. MGMT: its role in cancer aetiology and cancer therapeutics. *Nat Rev Cancer.* 2004; 4:296–307. [PubMed: 15057289]
19. Baldwin EL, Osheroff N. Etoposide, topoisomerase II and cancer. *Curr Med Chem Anticancer Agents.* 2005; 5:363–72. [PubMed: 16101488]
20. Wu J, Liu LF. Processing of topoisomerase I cleavable complexes into DNA damage by transcription. *Nucleic Acids Res.* 1997; 25:4181–6. [PubMed: 9336444]
21. Ju BG, Lunnyak VV, Perissi V, Garcia-Bassets I, Rose DW, Glass CK, et al. A topoisomerase IIbeta-mediated dsDNA break required for regulated transcription. *Science.* 2006; 312:1798–802. [PubMed: 16794079]
22. Dimri GP, Lee X, Basile G, Acosta M, Scott G, Roskelley C, et al. A biomarker that identifies senescent human cells in culture and in aging skin in vivo. *Proc Natl Acad Sci USA.* 1995; 92:9363–7. [PubMed: 7568133]
23. Komarov PG, Komarova EA, Kondratov RV, Christov-Tselkov K, Coon JS, Chernov MV, et al. A chemical inhibitor of p53 that protects mice from the side effects of cancer therapy. *Science.* 1999; 285:1733–7. [PubMed: 10481009]
24. Batista LF, Roos WP, Christmann M, Menck CF, Kaina B. Differential sensitivity of malignant glioma cells to methylating and chloroethylating anticancer drugs: p53 determines the switch by regulating xpc, ddb2 and DNA double-strand breaks. *Cancer Res.* 2007; 67:11886–95. [PubMed: 18089819]
25. Van Meir EG, Kikuchi T, Tada M, Li H, Diserens AC, Wojcik BE, et al. Analysis of the p53 gene and its expression in human glioblastoma cells. *Cancer Res.* 1994; 54:649–52. [PubMed: 8306326]



26. Jia LQ, Osada M, Ishioka C, Gamo M, Ikawa S, Suzuki T, et al. Screening the p53 status of human cell lines using a yeast functional assay. *Mol Carcinog.* 1997; 19:243–53. [PubMed: 9290701]
27. Bartkova J, Horejsí Z, Koed K, Krämer A, Tort F, Zieger K, et al. DNA damage response as a candidate anti-cancer barrier in early human tumorigenesis. *Nature.* 2005; 434:864–70. [PubMed: 15829956]
28. Lin AW, Barradas M, Stone JC, van Aelst L, Serrano M, Lowe SW. Premature senescence involving p53 and p16 is activated in response to constitutive MEK/MAPK mitogenic signaling. *Genes Dev.* 1998; 12:3008–19. [PubMed: 9765203]
29. Alcorta DA, Xiong Y, Phelps D, Hannon G, Beach D, Barrett JC. Involvement of the cyclin-dependent kinase inhibitor p16 (INK4a) in replicative senescence of normal human fibroblasts. *Proc Natl Acad Sci USA.* 1996; 93:13742–7. [PubMed: 8943005]
30. Reznikoff CA, Yeager TR, Belair CD, Savelieva E, Puthenveetil JA, Stadler WM. Elevated p16 at senescence and loss of p16 at immortalization in human papillomavirus 16 E6, but not E7, transformed human uroepithelial cells. *Cancer Res.* 1996; 56:2886–90. [PubMed: 8674033]
31. Quick QA, Gewirtz DA. An accelerated senescence response to radiation in wild-type p53 glioblastoma multiforme cells. *J Neurosurg.* 2006; 105:111–8. [PubMed: 16871885]
32. Zhou Q, Guo P, Kruh GD, Vicini P, Wang X, Gallon JM. Predicting human tumor drug concentrations from a preclinical pharmacokinetic model of temozolomide brain disposition. *Clin Cancer Res.* 2007; 13:4271–9. [PubMed: 17634557]
33. Kurose A, Tanaka T, Huang X, Halicka HD, Traganos F, Dai W, et al. Assessment of ATM phosphorylation on Ser-1981 induced by DNA topoisomerase I and II inhibitors in relation to Ser-139-histone H2AX phosphorylation, cell cycle phase and apoptosis. *Cytometry A.* 2005; 68:1–9. [PubMed: 16184611]
34. Tanaka T, Kurose A, Huang X, Dai W, Darzynkiewicz Z. ATM activation and histone H2AX phosphorylation as indicators of DNA damage by DNA topoisomerase I inhibitor topotecan and during apoptosis. *Cell Prolif.* 2006; 39:49–60. [PubMed: 16426422]
35. Darzynkiewicz Z, Bedner E, Traganos F. Difficulties and pitfalls in analysis of apoptosis. *Methods Cell Biol.* 2001; 63:527–59. [PubMed: 11060857]
36. Hirose Y, Katayama M, Mirzoeva OK, Berger MS, Pieper RO. Akt activation suppresses Chk2-mediated, methylating agent-induced G<sub>2</sub> arrest and protects from temozolomide-induced mitotic catastrophe and cellular senescence. *Cancer Res.* 2005; 65:4861–9. [PubMed: 15930307]
37. Hermisson M, Klumpp A, Wick W, Wischhusen J, Nagel G, Roos W, et al. O<sup>6</sup>-methylguanine DNA methyltransferase and p53 status predict temozolomide sensitivity in human malignant glioma cells. *J Neurochem.* 2006; 96:766–76. [PubMed: 16405512]
38. Xu GW, Mymryk JS, Cairncross JG. Pharmaceutical-mediated inactivation of p53 sensitizes U87MG glioma cells to BCNU and temozolomide. *Int J Cancer.* 2005; 116:187–92. [PubMed: 15800902]
39. Natsume A, Ishii D, Wakabayashi T, Tsuno T, Hatano H, Mizuno M, et al. IFN $\beta$  down-regulates the expression of DNA repair gene MGMT and sensitizes resistant glioma cells to temozolomide. *Cancer Res.* 2005; 65:7573–9. [PubMed: 16140920]
40. Hegi ME, Diserens AC, Gorlia T, Hamou MF, de Tribolet N, Weller M, et al. MGMT gene silencing and benefit from temozolomide in glioblastoma. *N Engl J Med.* 2005; 352:997–1003. [PubMed: 15758010]
41. Brell M, Tortosa A, Verger E, Gil JM, Viñolas N, Villá S, et al. Prognostic significance of O<sup>6</sup>-methylguanine-DNA methyltransferase determined by promoter hypermethylation and immunohistochemical expression in anaplastic gliomas. *Clin Cancer Res.* 2005; 11:5167–74. [PubMed: 16033832]
42. Pollack IF, Hamilton RL, Sobol RW, Burnham J, Yates AJ, Holmes EJ, et al. O<sup>6</sup>-methylguanine-DNA methyltransferase expression strongly correlates with outcome in childhood malignant gliomas: results from the CCG-945 Cohort. *J Clin Oncol.* 2006; 24:3431–7. [PubMed: 16849758]
43. Hunter C, Smith R, Cahill DP, Stephens P, Stevens C, Teague J, et al. A hypermutation phenotype and somatic MSH6 mutations in recurrent human malignant gliomas after alkylator chemotherapy. *Cancer Res.* 2006; 66:3987–91. [PubMed: 16618716]

44. Maxwell JA, Johnson SP, McLendon RE, Lister DW, Horne KS, Rasheed A, et al. Mismatch repair deficiency does not mediate clinical resistance to temozolomide in malignant glioma. *Clin Cancer Res.* 2008; 14:4859–68. [PubMed: 18676759]

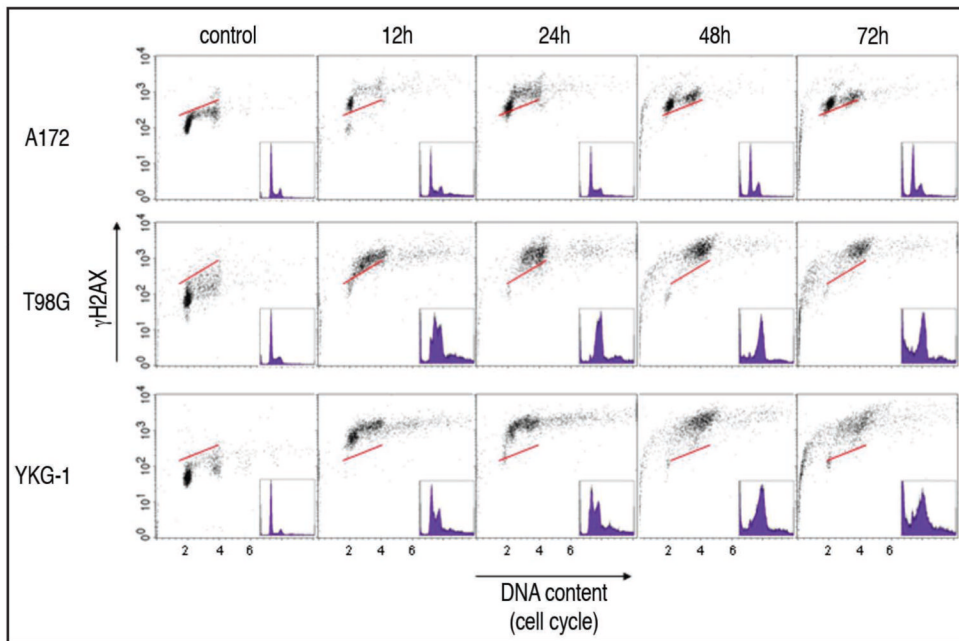


**Figure 1.**

Bivariate distributions (DNA content vs.  $\gamma$ H2AX) of glioblastoma cell lines, A172, T98G and YKG-1 treated with 23.5  $\mu$ g/ml etoposide for time intervals as indicated. The solid skewed lines indicate the upper level of  $\gamma$ H2AX immunofluorescence for 95% of cells in the untreated (control) culture. All the 3 types of cells demonstrate high level of  $\gamma$ H2AX through the cell cycle 12 h after the treatment. After 48 h, significant fraction of cells, greater in T98G and YKG-1 than A172 cultures, undergoes apoptosis.

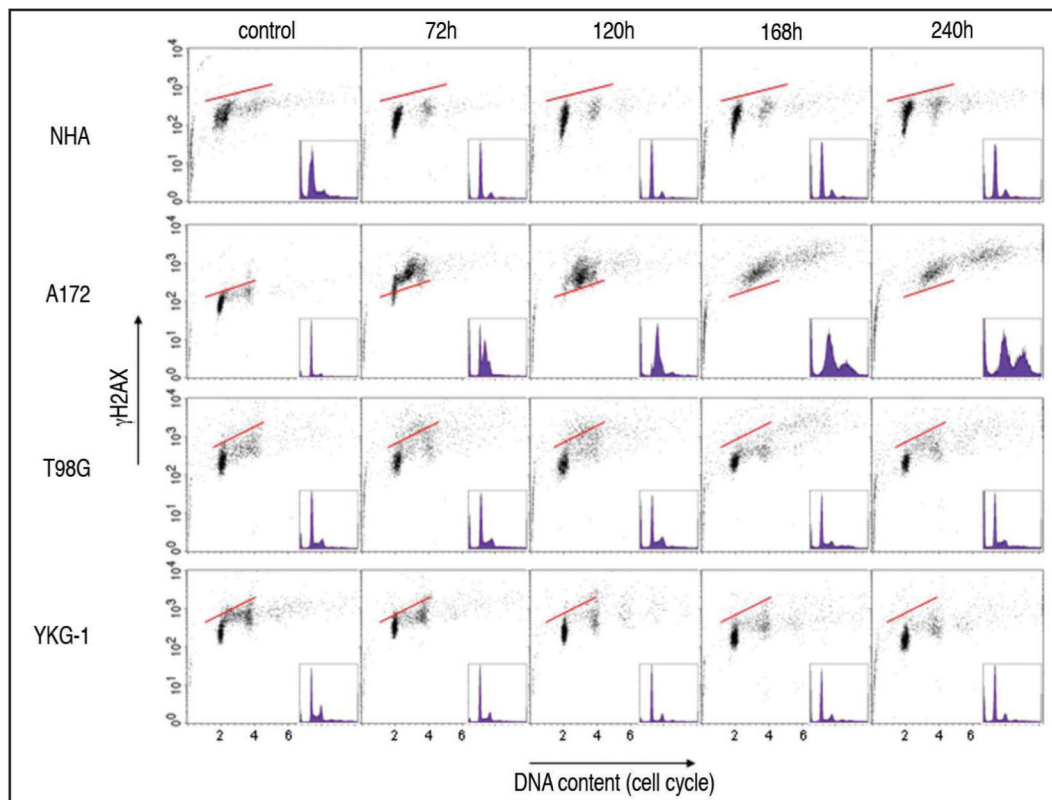


**Figure 2.**

Bivariate distributions (DNA content vs.  $\gamma$ H2AX) of NHA and glioblastoma cell lines, A172, T98G and YKG-1 after treatment with 100  $\mu$ M TMZ for time intervals as indicated. The solid skewed lines indicate the upper level of  $\gamma$ H2AX immunofluorescence for 95% of cells in the untreated (control) culture. Note accumulation of cells in G<sub>1</sub> and G<sub>2</sub>/M in NHA cultures with no evidence of  $\gamma$ H2AX induction, perturbed S- and G<sub>2</sub>/M-phase progression of A172 cells with high level of  $\gamma$ H2AX induction, transient (72 h-120 h) induction of  $\gamma$ H2AX in S phase of T98G cells, and modest degree of G<sub>1</sub> arrest with minimal induction of  $\gamma$ H2AX in YKG-1 cells. Relatively small number of apoptotic cells with fractional DNA content is apparent in cultures of all four cell lines.

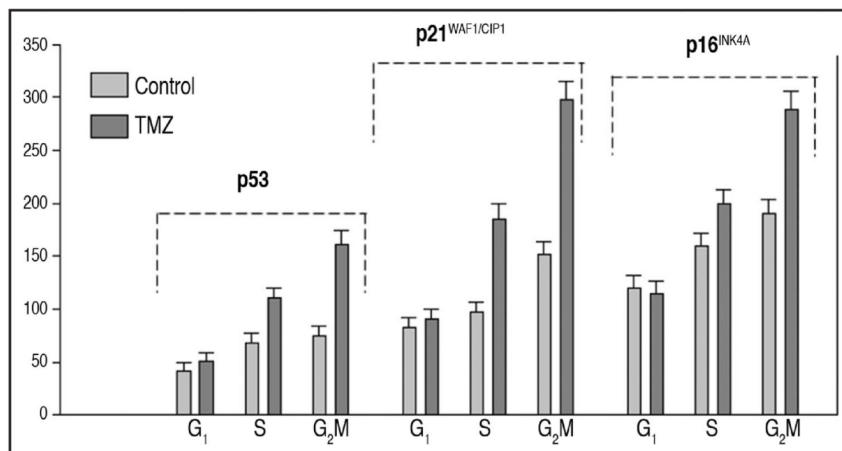


**Figure 3.** Effect of TMZ on expression of p53, p21<sup>WAF1/CIP1</sup> and p16<sup>INK4A</sup> in A172 cells in relation to the cell cycle phase. Untreated (control) and TMZ-treated (100  $\mu$ M, 120 h) cells were immunostained for p53, p21<sup>WAF1/CIP1</sup> and p16<sup>INK4A</sup> and their immunofluorescence was measured in conjunction with cellular DNA content by flow cytometry. Based on differences in cellular DNA content the cells in G<sub>1</sub>, S and G<sub>2</sub>/M were gated during analysis and their mean immunofluorescence (+SD, estimated based on Poisson distribution) was plotted in form of the bar-graphs (Sigma-plot).



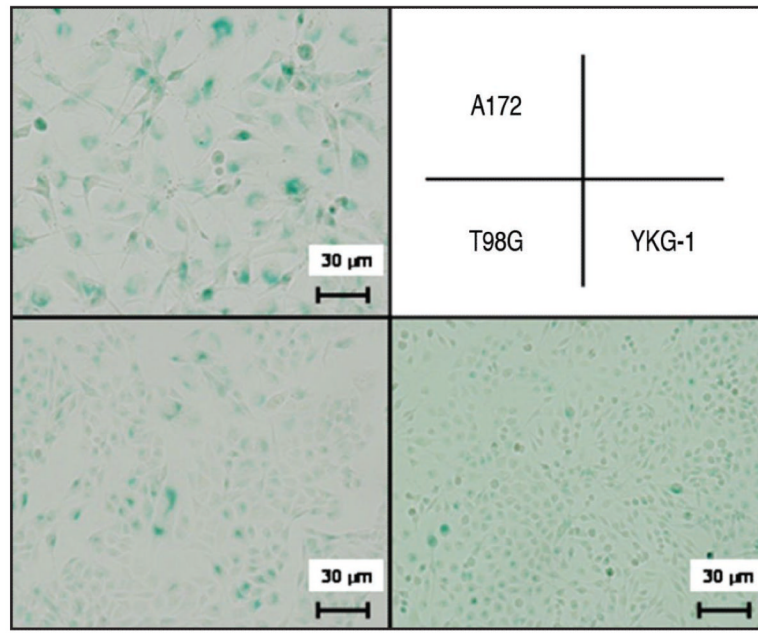


**Figure 4.**

Senescence-associated  $\beta$ -galactosidase staining in the glioblastoma cell lines after treatment with 100  $\mu$ M TMZ for 168 h. Blue color in the cytoplasm indicates senescence-associated  $\beta$ -galactosidase. After the treatment, 70% of A172 cells were positive for senescence-associated  $\beta$ -galactosidase whereas 20% of T98G and YKG-1 cells respectively were positive. Moreover, A172 cells become enlarged and flattened. All photographs were taken with the same magnification.